Hypoxia drives murine neutrophil protein scavenging to maintain central carbon metabolism

JCI The Journal of Clinical Investigation

Hypoxia drives murine neutrophil protein scavenging to maintain central carbon metabolism

Emily R. Watts, … , Moira K.B. Whyte, Sarah R. Walmsley

J Clin Invest. 2021. https://doi.org/10.1172/JCI134073.

Research In-Press Preview **Inflammation** **Metabolism**

Graphical abstract

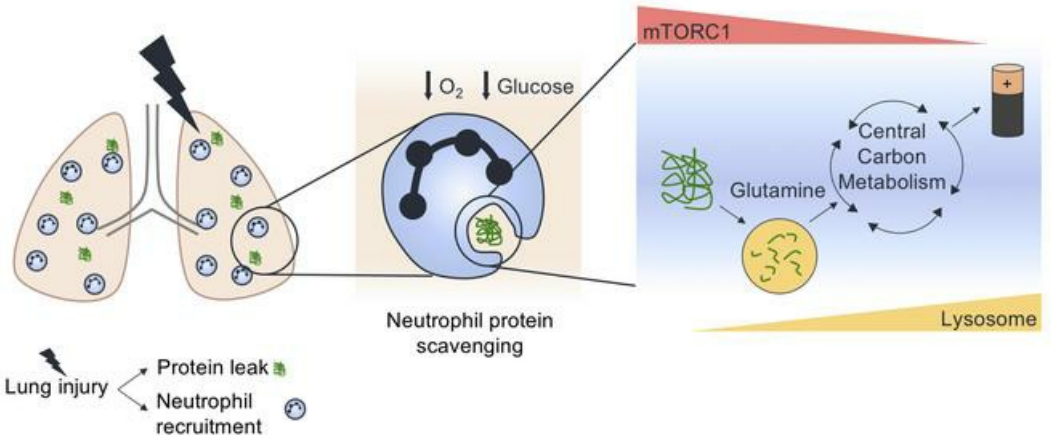

Hypoxia drives murine neutrophil protein scavenging to maintain central carbon metabolism

Emily R. Watts[1], Andrew J.M. Howden[2], Tyler Morrison[1], Pranvera Sadiku[1], Jens Hukelmann[2], Alex von Kriegsheim[3], Bart Ghesquiere[4], Fiona Murphy[1], Ananda S Mirchandani[1], Duncan C. Humphries[1], Robert Grecian[1], Eilise M Ryan[1], Patricia Coelho[1], Gio Rodriguez Blanco[3], Tracie M Plant[1], Rebecca S Dickinson[1], Andy Finch[3], Wesley Vermaelen[4], Doreen A. Cantrell[2], Moira K. Whyte[1], Sarah R. Walmsley[1*]

[1]University of Edinburgh Centre for Inflammation Research, Queen's Medical Research Institute, University of Edinburgh, Edinburgh, UK, EH16 4TJ.

[2]Division of Cell Signalling and Immunology, University of Dundee, Dundee, UK.

[3] Edinburgh Cancer Research Centre, IGMM, University of Edinburgh, Edinburgh, UK.

[4]Laboratory of Angiogenesis and Vascular Metabolism, Vesalius Research Centre, Leuven, Belgium.

*Corresponding author. Email: sarah.walmsley@ed.ac.uk, telephone 0131 242 6785.

Abstract:

Limiting dysfunctional neutrophilic inflammation whilst preserving effective immunity requires a better understanding of the processes that dictate neutrophil function in the tissues. Quantitative mass-spectrometry identified how inflammatory murine neutrophils regulated expression of cell surface receptors, signal transduction networks and metabolic machinery to shape neutrophil phenotypes in response to hypoxia. Through the tracing of labelled amino acids into metabolic enzymes, pro-inflammatory mediators and granule proteins we demonstrated that ongoing protein synthesis shapes the neutrophil proteome. To maintain energy supplies in the tissues, neutrophils consumed extracellular proteins to fuel central carbon metabolism. The physiological stresses of hypoxia and hypoglycaemia, characteristic of inflamed tissues, promoted this extra-cellular protein scavenging with activation of the lysosomal compartment further driving exploitation of the protein rich inflammatory milieu. This study provides a comprehensive map of neutrophil proteomes, analysis of which has led to the identification of active catabolic and anabolic pathways which enable neutrophils to sustain synthetic and effector functions in the tissues.

Introduction:

The rapid recruitment of innate immune cells is critical for containing and eradicating infection and the restoration of normal tissue homeostasis. To enable effective immune responses in the tissues, leukocytes are required to adapt to the physiological challenges provided by the inflammatory niche. This is reflected in the ability of neutrophils to survive and function under conditions of limited oxygen availability(1-3). Hypoxia in the context of pneumonia is associated with poorer outcomes in patients(4, 5) and we have previously shown that in murine models of bacterial pneumonia increased sickness in hypoxia is neutrophil-dependent(6). Furthermore, myeloid cell specific loss of the critical oxygen

sensing prolyl hydroxylase PHD2 resulted in a damaging inflammatory neutrophil phenotype in sterile and infective models of inflammation (7). Hypoxia is therefore an important determinant of neutrophil behaviour.

Variations in both local and systemic tissue oxygenation may be amplified in disease, for example in acute respiratory distress syndrome (ARDS) and more recently in COVID-19 disease. In both contexts, worsening hypoxia and alveolar damage is associated with increased mortality(8-10). Infiltrating neutrophils in the setting of ARDS drive an overexuberant inflammatory response which is highly damaging to host tissue(8), increasing vascular injury and protein leak(9, 10) and promoting the alveolar epithelial injury that dictates disease progression(11-13).

The release of granule proteases at the site of injury or infection represents a key component of the neutrophil's antimicrobial repertoire and these proteases are known to contribute significantly to tissue damage in ARDS(14). To facilitate the rapid release of these proteins, granules and their contents are preformed and packaged during neutrophil maturation in the bone marrow through a temporally regulated programme of transcription and translation (15, 16). Degranulation is necessarily a highly regulated process as inappropriate release of these toxic proteins risks host cell and tissue damage. The ability of neutrophils to sustain damaging, pro-inflammatory responses in oxygen and nutrient limited tissues raises the important possibility that neutrophils continue to synthesise destructive granule proteases.

Here we used a lung injury model to interrogate the processes which drive harmful neutrophil phenotypes. Quantitative label free mass-spectrometry revealed that inflammatory neutrophils have a dynamic proteome which is re-structured in response to the physiological stress of hypoxia. Tracing of labelled amino acids and proteins identified the capacity of airway neutrophils to undergo de novo protein synthesis and activate lysosomal functions required to metabolise extracellular proteins to fuel this response. Consistent with this

finding, systemic hypoxia aggravates lung injury, a response curtailed by lysosomal inhibition. This immune-metabolic leukocyte phenotype is of likely importance in both health and disease.

Results:

Inflammatory neutrophils re-structure their proteome in response to hypoxia

We firstly sought to develop a comprehensive map of the proteome of an inflammatory neutrophil to assess their capacity to respond to different environments and stimuli, something a genomics approach could not address. Moreover, the quantification of absolute protein abundance allows the unbiased analysis of the factors which differentiate the normoxic from the hypoxic neutrophil population.

Mice were exposed to nebulised lipopolysaccharide (LPS) using a sealed system to generate a uniform and reproducible lung injury. Airspace neutrophils were isolated from bronchoalveolar lavage (BAL) of mice 24 hours after induction of lung injury. Using high resolution mass spectrometry, we identified 57 000 peptides from these highly pure neutrophil preparations (Figure S1A-B), corresponding to over 5000 proteins. High correlation between biological replicates was observed (R^2>0.96, Figure S1C). Protein copy numbers were calculated on Perseus software(17) using the proteomic ruler(18) and used to analyse the contribution of proteins to the total protein mass (Figure S1D). Proteins were divided into quartiles by abundance (measured by label free quantification (LFQ) intensity) and the top 2 quartiles were analysed for KEGG pathway enrichment (as compared to the whole neutrophil proteome) using online DAVID software(19, 20). This analysis of the most abundant proteins highlighted that metabolic, migratory, inflammatory and biosynthetic pathways dominate the inflammatory neutrophil proteome (Figure 1A-B), with 7% total

protein mass attributable to glycolysis, 6% to regulation of translation and 5% to granule proteins (Figure 1C-E). Enrichment of inflammatory, metabolic and biosynthetic pathways was observed in neutrophils relative to the whole murine genome (Tables S1-3). We next questioned how neutrophils restructure their proteome in response to the physiological challenge of hypoxia and low glucose availability, to which neutrophils are subjected in vivo. Given existing evidence that oxygen availability critically regulates innate immune responses to lung injury and infection(6, 7), we studied a model of hypoxic acute lung injury. Following nebulisation (as described above), animals were transferred to a hypoxic chamber where the inhaled oxygen concentration is reduced to 10% over 1 hour. Proteomic analysis revealed a distinct protein signature in neutrophils from mice exposed to concurrent systemic hypoxia as compared to those from normoxic controls during acute lung injury (Figure 1F), with upregulation of 272 proteins and down regulation of 230 proteins ($P<0.05$, FDR 0.05, $S_0=0.1$, Figure 1G). Hypoxic samples also showed high correlation between biological replicates (Figure S1E)

Hypoxic neutrophils upregulate inflammatory receptors and translational machinery

Analysis of those proteins which were significantly upregulated in hypoxia revealed a number of key inflammatory receptors. Formylated peptide receptor (FPR) signalling is implicated in the regulation of neutrophil chemotaxis, degranulation, ROS production and transcriptional regulation(21). Both FPR1 and FPR2 were significantly upregulated in the proteome of hypoxic neutrophils (Figure 2A). TNF-α signaling is implicated in neutrophil adhesion(22), priming(23) and apoptosis(24). TNF-α is detected in the BAL supernatant following LPS induced lung injury (Figure S2A) and hypoxic airspace neutrophils displayed higher levels of TNFRSF1b (TNF receptor 2) protein (Figure 2B). Flow cytometry confirmed higher surface expression of TNFRSF1b on hypoxic neutrophils harvested 24 hours post-LPS

(Figure S2B). TNF receptor 1 was not identified on the neutrophil proteome but could be measured by flow cytometry. This identified a distinct pattern of expression with higher levels in hypoxia at 6 hours post-LPS but equivalent expression by 24 hours (Figure S2C). Thus, hypoxia may regulate neutrophil response to TNF-α through dynamic regulation of surface receptor expression.

One of the most upregulated proteins in the hypoxic neutrophil proteome was the beta component of the GM-CSF receptor (CSF2RB, Figure 2C). Ligation of the GM-CSF receptor results in wide ranging inflammatory neutrophil responses, including priming, degranulation(25) and survival(26). Flow cytometry confirmed BAL neutrophil surface expression of both the α and β subunit of this heterodimeric receptor. Both subunits were upregulated in hypoxia 6 hours post-LPS with equivalent surface expression between groups by 24 hours (Figure S2D-E). This hypoxic induction of GM-CSF receptor surface expression early in the inflammatory response is associated with increased neutrophil degranulation *in vivo* at 6 hours with significantly higher levels of elastase activity (Figure 2D) and MMP9 (Figure 2E) in hypoxic BAL supernatant. Degranulation is maximal at this early time point with levels of both elastase and MMP9 in the BAL falling by 24 hours (Figure S3A-B).

Despite detection of free elastase and MMP9 in the airways, the proteomic dataset showed that airspace neutrophils retain high protein expression of azurophilic, specific and gelatinase granule proteins (Figure 2F), and showed no reduction in intracellular levels of the key granule proteins under conditions of hypoxia (Figure 2G-H and Figure S3C-D) where enhanced degranulation is observed. Persistence of granule proteins in hypoxic neutrophils despite evidence of increased degranulation led us to hypothesise that tissue neutrophils may have the capacity to synthesise granule proteins upon recruitment to the inflammatory niche, in contrast to the existing dogma that granule proteins are only synthesised and packaged in bone marrow neutrophils(15). Consistent with this possibility, hypoxia positively regulated

many eukaryotic translation initiation factors (EIFs, essential for initiation of protein translation, (Figure 2I) and aminoacylation of tRNAs (Figure 2J-K). Furthermore, airspace neutrophils retain mRNAs for granule proteins (Figure S3E-F).

Airspace neutrophils synthesise granule proteins

To directly address the extent to which tissue neutrophils continue to synthesise inflammatory proteins, we measured the protein synthetic capacity of inflammatory BAL neutrophils by *ex vivo* incubation of BAL neutrophils with the heavy labelled amino acids $^{13}C_6$ and $^{15}N_4$ L-arginine and $^{13}C_6$ L-Lysine. BAL neutrophils from animals which had been housed in hypoxia following LPS stimulation were used because we predicted, based on the proteomic data presented here, that these would have the greatest capacity for ongoing protein synthesis. Neutrophils were isolated 6 hours after LPS nebulisation and cultured with heavy labelled amino acids for 18 hours to generate samples equivalent to those isolated 24 hours post LPS. 62 newly synthesised (labelled) proteins were identified by mass spectrometry including abundant proteins involved in cytoskeletal regulation and metabolism (Figure 3A and Table S5) as would be predicted from our initial proteomic screens (Figure 1B-C). Importantly we also identified labelling within inflammatory proteins such as complement C3 and integrins (Figure 3B) and granule proteins (27) (Figure 3C). De novo protein synthesis contributed significantly to the overall abundance of these granule proteins, with up to 10% heavy label incorporation. Coupled with the evidence of preserved intracellular granule proteins despite enhanced degranulation, this data is consistent with de novo synthesis of inflammatory mediators, including granule proteins by tissue neutrophils, providing a mechanism by which hypoxic neutrophils would be predicted to drive a hyper-inflammatory immune response.

Neutrophils scavenge extracellular proteins for fuel

Despite their well-recognised reliance on glycolysis for ATP production, we found that airway neutrophils are subject to significant hypoglycaemia. Only very low levels of glucose were present in BAL supernatant (Figure S4A) (28, 29). In order to more accurately determine the absolute concentration of glucose which cells within the airways are exposed to (without the diluting effect of the BAL) we also performed LCMS analysis of airway surface liquid which was adsorbed onto filter cards directly from the upper airways. This confirmed low levels of glucose in the airways of both normoxic and hypoxic mice (Figure 4A). Although hypoxic neutrophils did upregulate the glucose transporter Glut 3 (Figure 4B), this did not translate to an increase in intracellular glucose-6-phosphate (Figure 4C), likely due to the low substrate availability. We therefore asked how airway neutrophils are able to support the observed synthetic function in this metabolite deplete environment. In contrast to intracellular glucose levels, hypoxic neutrophils were found to have significantly higher levels of intracellular glutamine and glutamate (Figure 4D). LCMS analysis of airway fluid did detect glutamine, but there was no increase in hypoxic airways (Figure 4E). Furthermore, at a protein level, neutrophils did not reproducibly express the important SLC-38 family of glutamine transporters (Figure S4B) (30), suggesting that transport of free glutamine does not account for the observed increase in intracellular glutamine in hypoxia.

Survey of the neutrophil proteome led to the surprising observation that neutrophils contain the extracellular proteins albumin, IgM and fibronectin, and that they increase in abundance when neutrophils are exposed to hypoxic lung injury (Figure 4F-H). This led us to question whether neutrophils can scavenge proteins to use as an alternative source of amino acids, a mechanism employed by tumour cell lines to meet their increasing metabolic demands (31-33). Consistent with glutamine being an important metabolic substrate(34), a number of key enzymes and transporters involved in glutaminolysis (glutaminase, glutamate dehydrogenase,

alpha ketoglutarate dehydrogenase, phosphoenolpyruvate carboxykinase 2 and the dicarboxylate transporter) are upregulated at the protein level in hypoxia (Figure 5A). The ability of neutrophils to use an active protein uptake pathway to fuel their energetic requirements at sites of inflammation would represent an advantageous metabolic adaptation to the inflamed lung niche.

To definitively address whether neutrophils can use extracellular proteins for anaplerosis, we fed ex-vivo airspace neutrophils with $^{13}C_5$ glutamine labelled proteins and traced the presence of heavy carbons into their metabolic intermediaries. Label could be traced into TCA cycle metabolites including citrate, fumarate and malate (Figure 5B-D and Figure S4C-F), consistent with flux of protein-derived glutamine into central carbon metabolism. We did not identify any evidence of reductive carboxylation with no m+5 citrate (Figure S4C) and no m+3 malate (Figure S4D) identified. These experiments do not allow us to conclusively comment upon TCA cycling, whilst we did identify the presence of small amounts of m+2 citrate, we did not see labelling within oxaloacetate (data not shown). Neutrophils therefore have the capacity to utilise extracellular proteins as an amino acid source for metabolic intermediaries.

Hypoxia and mTORC1 activity regulate neutrophil catabolism of scavenged extracellular proteins

To investigate the use of extracellular proteins by neutrophils, we used Texas Red labelled bovine serum albumin (BSA) to measure protein uptake and double-quenched (DQ)-Green labelled BSA (which requires proteolytic cleavage to emit green fluorescence) to measure breakdown. We used human blood neutrophils in additional to murine BAL neutrophils to confirm that protein scavenging is of functional relevance in a broader range of neutrophil

subsets. Incubation of healthy human peripheral blood neutrophils with Texas Red BSA demonstrates rapid uptake with a significant increase in Texas Red signal after a 30 minute incubation (Figure 6A). Rapid proteolysis also occurs with a significant increase in the DQ-Green signal observed after 90 minutes (Figure 6A). To confirm that the observed DQ-Green signal was a direct result of intracellular proteolysis, rather than extracellular proteolysis and uptake of unquenched fluorescent BSA, the DQ-Green BSA time course was repeated following a wash at 30 minutes to remove residual extracellular albumin. Consistent with intracellular breakdown of DQ-Green BSA there was a significant increase in intracellular fluorescence over a 2-hour incubation period with fresh media (Figure 5B).

In order to delineate the mechanism by which neutrophils take up albumin, we used confocal microscopy to assess localisation of FITC-BSA and Texas-red 70kDa dextran, a substance predominantly taken up via macropinocytosis(35). Merged images revealed partial co-localisation of the BSA signal with the 70kDa dextran (Figure 6C) indicative that one route of albumin uptake is via macropinocytosis(36).

We hypothesised that in neutrophils, nutrient availability may play a role in regulating protein uptake. In light of the glucose deplete nature of the inflamed airway, we incubated LPS treated human peripheral blood neutrophils in the presence or absence of glucose and compared normoxic (21% O_2) with hypoxic (1% O_2) culture. Comparing the signal from neutrophils incubated with Texas red BSA with those incubated with DQ-Green BSA identified an interesting distinction between conditions which favour uptake versus those which favour breakdown. In glucose replete media, hypoxia enhances albumin uptake. This trend is preserved in glucose depletion but is non-significant (Figure 6D). In both normoxia and hypoxia, the absence of glucose results in reduced uptake of albumin but this is significant only in hypoxia (Figure 6D). In contrast, hypoxia enhances albumin breakdown in both glucose replete and deplete conditions (Figure 6E) and glucose depletion does not limit

albumin breakdown. This suggests that the increase in albumin catabolism which is driven by hypoxia is sufficient to overcome any reduced substrate uptake due to glucose deprivation. This is illustrated by the ratio of DQ-Green to Texas red fluorescence in each condition which can be used as an indicator of the proteolytic activity of the cells. This showed that LPS stimulated neutrophils incubated in hypoxia without glucose (conditions most closely resembling the hypoxic airway) had significantly higher proteolytic capacity than in any other condition (Figure 6F). This is consistent with the hypothesis that in conditions of nutrient scarcity, neutrophils exploit their environment to scavenge alternative energy supplies in the form of protein, and that hypoxia positively regulates this process. In order to investigate the in vivo relevance of this observation, inflammatory BAL neutrophils from normoxic and hypoxic mice were cultured ex-vivo with Texas red BSA and DQ-Green BSA (with those from normoxic mice cultured in 21% oxygen and those from hypoxic mice cultured in 1% oxygen). In these ex-vivo cells, hypoxia drives both increased protein uptake and degradation (Figure 6G-H). Thus, transmigration into the alveolar space and/or exposure to the inflammatory milieu further augments neutrophil protein scavenging capacity. Measurement of cell culture supernatant fluorescence confirmed that the enhanced DQ Green signal in hypoxia did not represent enhanced extracellular DQ activation secondary to increased degranulation of neutrophil proteases (Figure 6I).

In tumour cells, the mammalian target of rapamycin (mTOR) and its associated complexes, mTORC1 and mTORC2, are essential in integrating signals regarding nutrient availability. Down-stream signalling then determines the cellular response to these signals in terms of transcription and translation of new proteins and in directing proliferation(32). Interestingly, data in fibroblasts showed that mTORC1 activity negatively regulated lysosomal degradation of proteins taken up from the environment(32). We speculated that there might also be an inverse correlation between mTORC1 activity and protein breakdown by neutrophils. Our

proteomic data confirmed that neutrophils express the key components of mTORC1, mTORC2 and the Ragulator complex proteins LAMTOR1-3 required for translocation of mTORC to the lysosomal membrane(37) (Figure S5A-B). The basal activity of mTORC1 in human peripheral blood neutrophils was analysed using the phosphorylation status of the downstream target S6 kinase (S6K). In unstimulated neutrophils, mTORC1 activity was low and LPS treatment resulted in a significant increase in phosphorylated S6K (Figure S5C). Oxygen and glucose availability dramatically altered the activity of mTORC1 in LPS treated human peripheral blood neutrophils with suppression of mTORC1 activity by both hypoxia and glucose deprivation (Figure 6J), an effect replicated in vivo with diminished expression of phosphorylated S6K in airspace neutrophils isolated from hypoxic mice (Figure 6K). To investigate whether mTORC activity directly regulates catabolism of extracellular proteins, human peripheral blood neutrophils were incubated with the mTORC inhibitor Rapamycin or with the mTORC activator MHY1485(38) prior to the addition of LPS and DQ-Green BSA. With mTORC inhibition we observed a significant increase in proteolysis (as measured by DQ-Green fluorescence) and with mTORC activation, a significant decrease (Figure 6L). Thus, mTORC activity inhibits breakdown of proteins in neutrophils and mTORC suppression under oxygen and glucose-deplete conditions relieves this inhibition.

Hypoxia upregulates lysosomal catabolism of extracellular protein by tissue neutrophils for anaplerosis

The lysosome is essential for cellular protein degradation. To investigate the importance of lysosomal trafficking for extracellular protein catabolism by neutrophils, we first verified the cellular localisation of scavenged albumin. Using confocal microscopy, we observed co-localisation of DQ-Green BSA with the lysosomal marker LAMP1 (Figure 7A). Thus, neutrophils have capacity to traffic proteins from the extracellular environment to the

lysosome. KEGG pathway analysis of those proteins upregulated by hypoxia at a proteomic level revealed enrichment for the lysosome pathway (fold enrichment 1.564, p=0.032), with more detailed analysis of known lysosomal proteins(39) confirming the majority of lysosomal pathway members to be upregulated by hypoxia (Figure 7B and Table S4). In the hypoxic inflamed airway, neutrophils can, therefore, upregulate both the lysosomal pathway (Figure 7B) and the enzymes required to metabolise the resultant free amino acids such as glutamine (Figure 5A). The importance of the lysosome for protein catabolism is further supported by the observation that a lysosomal protease inhibitor E64(32) (Figure 7C) and an inhibitor of lysosomal acidification chloroquine(40) (Figure 7D) diminish the ability of neutrophils to breakdown DQ-Green BSA in vitro. Furthermore, lysosomal proteins were accounted for 14% of newly synthesised proteins in the previous amino acid tracing experiments (Figure 3A), further highlighting the importance of this organelle in the inflammatory neutrophil. Neutrophils therefore have the capacity to regulate uptake and degradation of extracellular proteins via the lysosome to provide amino acids required for the provision of metabolic intermediaries. Hypoxia and glucose deprivation positively regulate these processes via mTOR and the lysosome.

Hypoxia promotes a damaging hyper-inflammatory neutrophil phenotype in vivo

In response to systemic hypoxia, we have observed that neutrophils restructure their proteome, enhance extracellular protein scavenging and that this is associated with increased inflammation within the tissues. To determine the biological consequences of these proteomic adaptations we explored the physiological outcomes of exposing mice to systemic hypoxia in the context of acute lung injury. Concurrent exposure of mice to LPS and hypoxia resulted in profound hypothermia over the first 24 hours (Figure 8A), a response replicated in the setting of bacterial pneumonia(6) and in keeping with a more severe inflammatory

response. In keeping with hypoxic upregulation of inflammatory receptors and degranulation (Figure 2A-E), analysis of the BAL fluid supernatant revealed an increase in lung injury demonstrated by significantly more capillary leak of albumin (Figure 8B) and IgM (Figure 8C) in hypoxia. The very high levels of intracellular albumin and IgM observed in hypoxia (Figure 4F-G) are therefore likely to be a consequence of both increased substrate availability and increased uptake. While we did demonstrate increased capacity for protein uptake in hypoxic BAL neutrophils (Figure 6G), this relatively modest increase is unlikely to be sufficient to overcome the nearly 3-fold increase in BAL albumin concentration in the lungs of hypoxic mice. The excess lung damage was independent of neutrophil number, with preserved BAL (Figure 8D) and interstitial (Figure 8E) neutrophil counts despite lower circulating neutrophil numbers (Figure 8F) in hypoxia. Evidence of increased sickness and more significant lung injury in response to hypoxia, together with in vivo evidence of activated neutrophil surface phenotypes (Figure 8G-H))(41, 42), confirm important biological consequences of the observed proteomic changes. In hypoxia, increased protein leak provides abundant substrate for the upregulated processes of protein scavenging and catabolism. De novo protein synthesis contributes to ongoing inflammatory mediator production (Figure 3) and, in hypoxia, increased granule protease release into the lung is associated with increased lung injury culminating in a vicious cycle of persistent inflammation.

To confirm the physiological relevance of lysosomal protein trafficking for inflammation outcomes, we explored the consequence of in-vivo administration of chloroquine in the LPS lung injury model. Administration of intra-peritoneal chloroquine(43, 44) resulted in a partial rescue of the hypothermia observed following LPS challenge (Figure 8I), without a reduction in neutrophil numbers (Figure 8J). When BAL neutrophils were cultured ex-vivo with DQ-Green albumin for two hours, as predicted from our in vitro treatment of human blood neutrophils, there was an associated reduction in DQ-Green fluorescence in airway

neutrophils harvested from the chloroquine treated mice, indicating that intra-peritoneal chloroquine is sufficient to reduce the lysosomal breakdown capacity of neutrophils recruited to the airways (Figure 8K). Moreover, analysis of the BAL supernatant showed a suppression of neutrophil granule protease production with a reduction in elastase activity in the airways of chloroquine treated mice (Figure 8L). Thus, systemic chloroquine treatment in mice leads to reduced neutrophil lysosomal activity and is associated with diminished release of neutrophil granule proteins in the airways. Further work will be required to delineate whether the observed effects of chloroquine relate directly to lysosomal inhibition and whether specific targeting of the lysosome can drive resolution of neutrophil mediated inflammatory lung disease.

Discussion:

The factors which tip the balance of neutrophil phenotype from functional immunity to pathological inflammation remain poorly understood. As a consequence, designing therapies for the many pathologies which are known to be mediated by neutrophilic inflammation remains a major challenge. Study of the proteome of the inflammatory neutrophil provides insights into the importance of biosynthesis for neutrophil function, with neutrophils demonstrating enrichment for the ribosome and RNA transport as well as inflammatory pathways. Comparison of normoxic and hypoxic neutrophil proteomes demonstrates that neutrophils have the capacity to re-structure their proteomes to adapt to physiological stressors and regulate these important biosynthetic functions. Exploring the biological consequence of these metabolic adaptations provides insights into the mechanisms by which neutrophils sustain their effector functions in the tissues.

Protein-rich exudates are pathognomonic of acute lung injury. In this work we observe that protein leak is not only a marker of lung damage but also has the capacity to drive further inflammation, with the finding that airspace neutrophils can take up extracellular proteins. We show for the first time that neutrophils not only scavenge proteins from their environment but use these ingested proteins to contribute amino acids to maintain central carbon metabolism. Moreover, this response is quick, with lysosomal breakdown of extracellular albumin occurring within 90 minutes and evidence of contribution to metabolite synthesis at 18 hours. This is consequently of biological importance given the predicted lifespan of tissue neutrophils following recruitment during an acute inflammatory response(45, 46) which is further extended by the presence of both tissue and systemic hypoxia(1, 7).

The hypoxic inflamed lung represents an optimal niche to increase neutrophil capacity for protein consumption, providing increased access to extracellular albumin and IgM, suppression of mTORC activity and promotion of lysosomal catabolism. We propose that initial hypoxic induction of formylated peptide, TNF-α and GM-CSF inflammatory receptors further provides a mechanism by which early neutrophil mediated damage and protein leak would provide substrate to fuel this continued inflammatory response.

The observation that, in hypoxia, high concentrations of granule proteases in the supernatants are not accompanied by reduced intracellular levels of these proteins led us to investigate whether tissue neutrophils continue to synthesise granule contents. Incorporation of labelled amino acids into newly synthesised granule proteins confirms their ongoing production by tissue neutrophils. We also provide direct evidence that neutrophils can release amino acids from scavenged proteins fuelling central carbon metabolism. These observations, in conjunction with our findings of increased levels of granule proteins in hypoxia, where proteins scavenging is also increased, raise the possibility that amino acids from scavenged proteins may also provide substrate for protein synthesis. The enhanced capacity for protein

translation observed in hypoxic neutrophils, coupled with increased protein substrate availability would support this concept. This hypothesis is further supported by the evidence that in vivo inhibition of lysosomal protein catabolism led to reduced neutrophil elastase production by airways neutrophils. Further work is required to confirm whether amino acids from scavenged proteins can be incorporated in newly synthesised proteins by neutrophils in the inflammatory niche.

There are clear parallels to be drawn between the harsh oxygen and glucose limited environment of the inflamed lung and the tumour microenvironment(47). Macropinocytosis of protein has been shown to be an important metabolic adaptation by tumour cells to metabolic stress(32, 33). In human blood neutrophils, the observed co-localisation of FITC-BSA with dextran and LAMP1 also highlights a role for macropinocytosis in the delivery of extracellular proteins to the neutrophil lysosome. It is unlikely that macropinocytosis reflects the only mechanism of protein uptake given the partial correlation of BSA with dextran and the capacity of neutrophils, as professional phagocytes, to ingest particles by a number of alternative routes.

The importance of extracellular protein uptake to the metabolic adaptations of neutrophils within the inflammatory niche was explored in a series of labelled protein tracing experiments. Our data provides direct evidence that immune cells are able to derive amino acids from proteins for central carbon metabolism. This substrate utilisation is promoted by hypoxic upregulation of the lysosomal compartment and concurrent suppression of mTORC1 activity, augmented by glucose deprivation, allowing unfettered catabolism of proteins in the lysosome. Increased expression of enzymes involved in glutaminolysis further supports metabolism of the resulting free amino acid pool in hypoxia facilitating anaplerosis. Neutrophils use gluconeogenesis to generate glycogen stores with glycogen cycling retaining energy production when extracellular glucose is limited(34). In this work, we propose that

glutamine derived from scavenged proteins feeds into this gluconeogenic response, generating ATP. It is interesting to speculate whether substrate-level phosphorylation at the level of succinate coA ligase could also be contributing to ATP production in this context. The inflammatory capability of neutrophils is not therefore limited to releasing proteases from preformed granules, but is dynamic and adapted to the inflammatory niche. Understanding the factors which regulate the capacity of neutrophils to synthesise and release granule proteins will be a significant focus moving forwards. Direct evidence of protein-derived amino acid incorporation into newly synthesised proteins has proved technically challenging but remains an area of active investigation. It is also interesting to speculate whether microenvironmental factors, including hypoxia and metabolic stress may shape the transcriptome of the neutrophil, determining the programme of protein synthesis, and whether the mechanism of release of these newly synthesised proteins is by further rounds of degranulation or involves alternative routes of exocytosis. This work has focussed on the breakdown of extracellular proteins but it is important to acknowledge that the closely related process of autophagy, whereby cells recycle intracellular proteins, may also contribute to the amino acid pool in the neutrophil. In future work, it will also be important to consider how the processes of transmigration and activation themselves alter the neutrophil proteome.

Given the frequency with which other inflamed tissues(48), including the bowel(49) and joint(50) are found to be hypoxic, the pathways identified here are likely to be relevant in regulation of neutrophilic inflammation more broadly. These data contribute to our understanding of the mechanisms by which neutrophils sense and adapt to local microenvironmental stresses, characteristic of the inflammatory niche and, as such, provide new strategies for the treatment of neutrophil mediated inflammatory disease.

Materials and Methods

Isolation and culture of human peripheral blood neutrophils

Human peripheral blood neutrophils were isolated from sodium citrate anticoagulated blood by dextran sedimentation and discontinuous Percoll as previously described(51). Purity was assessed by morphology on cytocentrifuge slides.

Murine LPS Induced acute lung injury

Mice were treated with lipopolysaccharide (LPS) from Pseudomonas aeruginosa 10 (1mg/ml, Sigma Aldrich) for 10 minutes using oxygen driven nebulisation into a custom-built sealed system to generate a uniform and reproducible acute lung injury(7, 52). Following LPS treatment, animals were housed in either normal room air or in hypoxia. Animals were culled using an overdose of intraperitoneal (IP) anaesthetic at the appropriate time point (2-48 hours post-nebulisation) and tissues harvested.

Exposure to Hypoxia

Mice were exposed to hypoxia (10% inspired O_2) in an InVivo Hypoxic Cabinet System (Coy Labs, USA) with excess CO_2 scavenged using Sofnolime soda lime chips (Molecular Products, UK) with colour indicator. In models of acute hypoxia, LPS stimulated or naïve mice were housed in hypoxia for 2-48 hours prior to tissue harvest.

Intraperitoneal chloroquine administration

Following administration of nebulised LPS, as described above, mice were housed in hypoxia or normoxia and at four hours were treated with intraperitoneal (IP) chloroquine diphosphate (Sigma Aldrich) at a dose of 50mg/kg diluted in PBS. Control mice were given IP PBS alone. Following chloroquine or PBS injection, animals were housed as before in either normoxia or hypoxia until being culled by overdose of intraperitoneal anaesthetic 24 hours post-LPS.

Murine neutrophil isolation

Bronchoalveolar lavage (BAL) neutrophils

The trachea was cannulated using a 24G cannula which was tied in place. The lungs were washed with 4ml of ice cold 0.9% NaCl and BAL fluid kept on ice until further processing. Cell counts were carried out using a haemocytometer and purity assessed by morphology on cytospin.

A discontinuous Percoll gradient (78%, 69% and 52% Percoll) was used to purify BAL neutrophils for RNA, protein and metabolite assays. Residual red blood cells were lysed by hypotonic saline lysis. Purity was assessed by morphology and flow cytometry with neutrophil purity>98%.

Murine Lung Digest

Following the BAL protocol described above, the right ventricle was cannulated, and the circulation flushed with 10ml of ice-cold PBS to minimise circulating leucocytes within the lung vasculature prior to lung harvest. The lung tissue was mechanically dissociated using scissors prior to enzymatic digestion with collagenase V (0.8mg/ml, Sigma-Aldrich), Collagenase D (0.625mg/ml, Roche), Dispase (1mg/ml, Gibco) and DNase (30μg/ml, Roche) made up in RPMI. The digest was then passed through a 100μm filter, washed with PBS and red cell lysis performed (Sigma Aldrich) prior to resuspension in FACS buffer (PBS with 5%BSA and 2mM EDTA). The cell suspension was passed through a 40μm filter, counted using a NucleoCounter automatic cell counter (Eppendorf) and processed for flow cytometry analysis.

Cell Culture

For all experiments, murine neutrophils were cultured at a density of $1x10^6$/ml and human neutrophils at a density of $5x10^6$/ml. Media was supplemented with 1% Penicillin Streptomycin (Gibco) and 10% dialysed FCS (Gibco) unless otherwise stated. Neutrophils

were cultured in RPMI 1640 media with 2mM glutamine (Gibco). The glucose replete media had 11mM D-glucose. Standard cell culture was carried out in a Thermo Scientific Heraeus BB15 CO2 incubator. For hypoxic cell culture, conditions were as above but cells were cultured in a Ruskin hypoxic work station (Ruskin, UK) with an O_2 of 1% and CO_2 of 5%. Humidity in the hypoxic work station was maintained at 70%.

HEK cell lysates were used as a substrate to analyse the downstream use of scavenged proteins. HEK 293 cells were a gift from Alex Von Kriegsheim (IGMM, University of Edinburgh). Control cells were cultured in glucose replete DMEM (Gibco) with 10% dialysed FCS, 1% Penicillin Streptomycin and 2mM L-glutamine. For glutamine labelling experiments, standard L-Glutamine was substituted with $^{13}C_5$ labelled Glutamine (Cambridge Isotopes, USA) for 72 hours prior to being harvested and lysed.

Acetone precipitation of HEK cell proteins

Cells were harvested and washed three times with ice-cold PBS. The cell pellet was then lysed by hypotonic lysis in 4ml of sterile water prior to sonication and acetone precipitation, with supernatants (containing small molecules such as metabolites and free amino acids) discarded. Samples were centrifuged at 13,000rpm for 10 minutes to remove insoluble protein material and supernatants utilised for downstream culture. Protein content was measured by Pierce BCA assay (Thermo Scientific) and normalised between labelled and unlabelled samples.

Ex-vivo culture of BAL neutrophils with glutamine labelled HEK cell proteins

BAL neutrophils were isolated and purified by Percoll gradient as detailed above. Following purification neutrophils were resuspended in glucose and glutamine free DMEM (Gibco) supplemented with 10% FCS and 400μg/ml of HEK cell protein isolated by acetone precipitation as above. Neutrophils were cultured at a density of $1x10^6$/ml for 18 hours in

hypoxia. Following this period of culture, cells were washed three times with sterile 0.9% NaCl prior to methanol lysis as detailed below.

HPLC-MS analysis of metabolites

Highly pure BAL neutrophils were analysed for intracellular metabolite abundance, either immediately following isolation or following culture with labelled HEK lysates. Following Percoll purification as described, cells were washed in ice cold 0.9% NaCl prior to resuspension in 80% Methanol. Following centrifugation at 20,000G for 10 minutes at 4°C pellets were retained, and protein content measured by Pierce BCA assay (Thermo Scientific). Samples were analysed at the VIB Center for Cancer Biology in Leuven using a Dionex UltiMate 3000 LC System (Thermo Scientific) coupled to a Q Exactive Orbitrap mass spectrometer (Thermo Scientific) operated in negative mode. Data collection was performed using Xcalibur software (Thermo Scientific). All data values were subsequently corrected for protein content based on the BCA assay.

Airway surface liquid was analysed by insertion of custom made filter cards (Hunt Developments, UK) into the upper airway of mice prior to bronchoalveolar lavage. Metabolites were subsequently eluted from the filter cards in 200 μL of 40:40:20 methanol:acetonitrile:water. Following extraction, samples were stored at –80 °C. Relative metabolite abundance was determined using ion-pairing Reverse Phase High Performance Liquid Chromatography (RP-HPLC) or Hydrophilic Interaction Liquid Chromatography coupled to a Q-Exactive Orbitrap Mass Spectrometer. Data were analysed in a targeted manner, using Xcalibur (Thermofisher Scientific) against an in-house compound library to integrate the area under the curve at the expected retention time and the average of two replicates subjected to analysis. In order to extrapolate absolute values for airway glucose and glutamine, a ‘standard curve’ was generated. The filter cards from the in vivo experiments were weighed to ascertain the mean volume of airway surface fluid which had been adsorbed

onto the card (6.4μL). An equivalent volume of either glucose or glutamine was applied to filter cards at varying concentrations and these samples were eluted and run in parallel with the experimental samples.

Sample preparation for proteomic analysis

Percoll purified BAL neutrophils were lysed in SDS lysis buffer with TCEP at a10mM working concentration and boiled for 5 minutes. Samples underwent 15 minutes of sonication then incubation with benzonase for 15 mins at 37°C. Protein concentration was estimated using the EZQ protein quantitation kit (Invitrogen). Following quantification, iodoacetamide (IAA) was added at a working concentration of 20mM and lysates incubated for 1 hour at room temperature. In-solution digestion was carried out using SP3 beads and LysC (overnight incubation at 37°C) at a concentration of 1μg LysC (Promega) per 100μg protein followed by trypsin (Promega) digestion, also at 1μg enzyme per 100μg protein overnight at 37°C. Peptides were eluted using acetonitrile (ACN) and quantified using the CBQCA assay. Samples were diluted to a concentration of 1μg/15μl with 5% formic acid and 1μg of peptide was submitted for fractionation. Samples were fractionated using strong anion exchange chromatography, analysed in an LTQ-Orbitrap Velos MS, and raw data processed using MaxQuant software(53). Subsequent statistical analysis and figure generation was carried out using Perseus software(17), Microsoft Excel and GraphPad Prism. The mass spectrometry proteomics data have been deposited to the ProteomeXchange Consortium via the PRIDE(54) partner repository with the dataset identifier PXD013672.

Neutrophil protein lysates

Isolated neutrophils were washed twice with cold PBS following culture or purification. Cells were pelleted by centrifugation at 300G for 5 minutes and the supernatant removed. The pellet was resuspended in Laemmli buffer with PMSF, phosphatase inhibitors and protease inhibitors (100μl Laemmli buffer per 1 million murine or 10 million human neutrophils). An

equal volume of 2x SDS lysis buffer was then added and mixed by pipetting. The sample was then boiled for 5 minutes prior to storage at -80°C until use.

Immunoblot for protein expression

Neutrophil protein lysates were analysed for protein expression by western blot. Proteins were separated by SDS-PAGE (8, 10 or 12% gels depending on protein size) using the BioRad mini-protean system prior to wet transfer onto PVDF membrane (Merck Millipore). Membranes were blocked using 5% skimmed milk powder for a minimum of 2 hours. Primary antibodies were from Cell Signalling Technology (p38 9212, P70 S6 Kinase 2708, Phospho-p70 S6 Kinase 9234, HRP linked anti-rat immunoglobulin 7077, HRP linked anti-mouse immunoglobulin 7076), Abcam (elastase Ab205670, MMP9 Ab58803, MPO Ab 188211) and Dako (HRP linked anti-rabbit immunoglobulin, p044801) and were made up in 5% skimmed milk in 1X TBS-Tween (TBST, 0.05% Tween). Membranes were incubated at 4°C overnight on a rolling platform. Membranes underwent three washes in 1X TBST prior to incubation with the appropriate horseradish peroxidase (HRP) conjugated secondary antibody for 1 hour at room temperature. The membrane was washed as above prior to developing in enhanced chemiluminescent (ECL) detection reagent (GE Healthcare). Chemiluminescence was assessed using a Licor Odyssey Fc machine and quantified using ImageStudioLite software. Protein quantification was normalised to a loading control as follows: The membrane was stripped using Restore Western Blot stripping buffer (Thermo Scientific), washed with dH_2O and then re-probed for the loading control protein (or, for the non-phosphorylated form of the protein of interest where appropriate) with primary and secondary antibodies as above. The membrane was then developed, and protein quantified as above.

Neutrophil RNA extraction and TaqMan analysis of gene expression

Percoll purified neutrophils were used to generate mRNA samples using the *mir*Vana miRNA isolation kit (Invitrogen) as per manufacturer instructions followed by DNase treatment using the Invitrogen TURBO DNA free kit. The quantity and purity of the RNA was assessed using a Nanodrop 100 spectrophotometer. cDNA was generated using AMV reverse transcriptase and random primers (Promega) and samples were run on a Techne Thermal cycler as follows: 23°C for 5 minutes, 42°C for 2 hours, 99°C for 2 minutes. Samples were stored at -20°C until use.

Gene expression was analysed using predesigned qPCR primer/probe assays from IDT, Leuven (*Elane* Mm.PT.58.6682392.gs, *MMP9* Mm.PT.58.10100097 and *MPO* Mm.PT.58.5251395) and Prime Time Gene Expression Mastermix (IDT, Leuven). For all assays, samples were run in triplicate and the gene of interest expressed relative to expression of a housekeeping gene (beta-actin, Mm.PT.39a.22214843.g). Assays were run on a 7900HT Fast real-time PCR system (Applied Biosystems). Data was analysed using SDS 2.0 software (Thermo Scientific).

Analysis of BAL supernatant

The first 0.8ml aliquot of BAL fluid was used to analyse the activity or quantity of a number of proteins and metabolites within the BAL fluid. The freshly isolated aliquot was kept on ice and centrifuged at 2000rpm for 10 minutes at 4°C to pellet the BAL leucocytes and erythrocytes present in the aliquot. The supernatant was removed into a fresh tube, flash frozen on dry ice and stored at -80°C until use. In all assays commercial kits were used as per the manufacturer protocol (IgM ELISA Abcam Ab133047, Albumin ELISA Abcam Ab108792, EnzCheck Elastase Activity Assay kit Invitrogen E12056, EnzCheck MPO Activity Assay kit Invitrogen E33856, MMP9 ELISA Bio-Techne MMPT90) and the optimal dilution of samples was pre-optimised for each different analyte.

Analysis of murine neutrophils by flow cytometry

300-500µl blood was collected into 30µl EDTA and underwent red cell lysis as described above. Cells were counted using a haemocytometer and $2x10^5$ cells were stained for flow cytometric analysis. Whole BAL was counted by haemocytometer and resuspended at a density of $1x10^6$ cells/ml. An aliquot of $2x10^5$ cells was then stained for analysis. Following digest as described above, $2x10^5$ cells were stained and analysed by flow cytometry.

Murine flow cytometry staining protocol

Viability assay: For lung digest samples only, samples were first resuspended in Live/Dead fixable Aqua stain (Invitrogen) as per manufacturer's protocol.

For all tissue types, samples were blocked in 25µl of PBS with 10% mouse serum and 1% Fc Block (Biolegend) for 15 minutes on ice. The antibody master mix was made up in PBS and 50µl of master mix was added to each sample. Cells were stained for 30 minutes on ice in the dark prior to being washed three times in FACS buffer and either being fixed in 4% PFA for 15 minutes at room temperature or analysed immediately on a BD LSR Fortessa cell analyser. For all flow cytometry experiments, data was acquired using FACS Diva software and analysed using FlowJo software (version 10.1). Flow cytometry antibodies are detailed in Table S6.

Dextran and albumin uptake assays

Neutrophils were pre-incubated in normoxia or hypoxia, in glucose deplete or replete media for 2 hours prior to the addition of Texas-Red labelled 70kDa dextran (Invitrogen), FITC or double quenched (DQ)-Green labelled BSA (Invitrogen) ± LPS (100ng/ml). E64 (2µM, Sigma-Aldrich), chloroquine (10µM, Sigma-Aldrich) rapamycin (50nM, Sigma-Aldrich) or the activator of mTOR MHY1485 (2µM Merck chemicals) were added for 1 hour prior to fluorescent albumin. Uptake was quantified by flow cytometry and localisation assessed by confocal microscopy.

Confocal microscopy

Confocal microscopy was used to delineate the intra-cellular location of the fluorescently labelled compounds described above. Neutrophils were washed and fixed in 4% PFA prior to permeabilisation with 0.1% Triton X100. The cells were washed again in PBS before staining with a deep-red cell mask (1μg/ml, Invitrogen). For LAMP1 co-localisation, cells were fixed using "cytofix/cytoperm" (BD Biosciences) and stained (LAMP1, Abcam mouse monoclonal) in 1x Perm/Wash buffer (containing FCS and saponin). Alexa Fluor 647 conjugated goat anti-mouse secondary antibody (Abcam) was used for detection, with pellets resuspended in ProLong Gold liquid mountant with DAPI for nuclear staining (Invitrogen). Confocal images were acquired using a Leica SP5 confocal laser scanning microscope with Leica Application Suite software.

Statistical Analysis

Graphs were created in GraphPad Prism 7, Microsoft Excel or Perseus(17). KEGG pathway enrichment analysis(19) was carried out using online DAVID ('database for annotation, visualization and integrated discovery') bioinformatics tools. A P value less than 0.05 was considered significant.

Study Approval

Mice

C57BL/6JOlA mice were purchased from Envigo, UK. Male mice aged 8-10 weeks were used in all experiments. All mouse experiments were conducted in accordance with the Home Office Animals (Scientific Procedures) Act of 1986 under a Home Office Project License (PPL 70/8364) with local ethics approval.

Healthy human blood

Human peripheral venous blood was taken from healthy volunteers with written informed consent as approved by the University of Edinburgh Centre for Inflammation Research Blood

Resource Management Committee (AMREC 15-HV-013). Volunteers were 61% female and aged 21-40 (55% in the 21-30 age bracket and 65% in the 31-40 age bracket).

Data Availability

The mass spectrometry proteomics data have been deposited to the ProteomeXchange Consortium via the PRIDE(54) partner repository with the dataset identifier PXD013672.

Author contributions:

E.R.W. performed experimental design, all experiments, data acquisition and interpretation. A.J.M.H. and J.H. performed proteomic data acquisition and interpretation. A.vK. performed amino acid tracing data acquisition and interpretation. B.G. and A.F. performed experimental design for metabolite data set acquisition. T.M. and P.S. performed data acquisition and interpretation of metabolic data sets. P.C., F.M, A.S.M, D.C.H., T.M.P. and R.S.D. performed in vivo data acquisition. W.V. and G.R.B. provided metabolic intermediary data acquisition. R.G. and E.M.R. assisted with in vitro assays. D.A.C. performed experimental design and conducted scientific direction. M.K.W. conducted scientific direction and wrote the manuscript. S.R.W. performed experimental design, data analysis and conducted scientific direction and wrote the manuscript.

Acknowledgments:

We are grateful to the MS facility at the College of Life Sciences of the University of Dundee and to the Mass Spectrometry and Proteomic Facilities at the Institute for Genetics and Molecular Medicine at the University of Edinburgh, We would like to thank the Flow Cytometry and Cell Sorting facility at the Queens Medical Research Institute, University of Edinburgh for their advice and assistance. We are very grateful to Prof Trevor Hansel and Dr Ryan Thwaites (Imperial College, London) for generously providing us with the filter cards for measurement of airway metabolites and for sharing their expertise to help with this work. Finally, we are grateful to the staff in the Bioresearch and Veterinary services department at

the Little France site, University of Edinburgh for all of their assistance with the animal work int his manuscript.

Funding: This work was supported by Wellcome Trust Clinical Fellowship awards (108717/Z/15/Z E.R.W., 098516 and 209220 S.R.W.).

Competing interests: The authors declare no competing interests.

References:

1. Walmsley SR et al. Hypoxia-induced neutrophil survival is mediated by HIF-1alpha-dependent NF-kappaB activity. *J. Exp. Med.* 2005;201(1):105–115.

2. Mecklenburgh KI et al. Involvement of a ferroprotein sensor in hypoxia-mediated inhibition of neutrophil apoptosis. *Blood* 2002;100(8):3008–3016.

3. Hannah S et al. Hypoxia prolongs neutrophil survival in vitro. *FEBS Lett.* 1995;372(2-3):233–237.

4. Majumdar SR, Eurich DT, Gamble J-M, Senthilselvan A, Marrie TJ. Oxygen saturations less than 92% are associated with major adverse events in outpatients with pneumonia: a population-based cohort study. *Clin. Infect. Dis.* 2011;52(3):325–331.

5. Sanz F et al. Hypoxemia adds to the CURB-65 pneumonia severity score in hospitalized patients with mild pneumonia. *Respir Care* 2011;56(5):612–618.

6. Thompson AAR et al. Hypoxia determines survival outcomes of bacterial infection through HIF-1alpha dependent re-programming of leukocyte metabolism. *Sci Immunol* 2017;2(8):eaal2861.

7. Sadiku P et al. Prolyl hydroxylase 2 inactivation enhances glycogen storage and promotes excessive neutrophilic responses. *J. Clin. Invest.* 2017;127(9):3407–3420.

8. Zemans RL, Matthay MA. What drives neutrophils to the alveoli in ARDS? *Thorax* 2017;72(1):1–3.

9. Flick MR, Perel A, Staub NC. Leukocytes are required for increased lung microvascular permeability after microembolization in sheep. *Circ. Res.* 1981;48(3):344–351.

10. Bachofen M, Weibel ER. Alterations of the gas exchange apparatus in adult respiratory insufficiency associated with septicemia. *Am. Rev. Respir. Dis.* 1977;116(4):589–615.

11. Dreyfuss D, Saumon G. Role of tidal volume, FRC, and end-inspiratory volume in the development of pulmonary edema following mechanical ventilation. *Am. Rev. Respir. Dis.* 1993;148(5):1194–1203.

12. Acute Respiratory Distress Syndrome Network et al. Ventilation with lower tidal volumes as compared with traditional tidal volumes for acute lung injury and the acute respiratory distress syndrome. *N. Engl. J. Med.* 2000;342(18):1301–1308.

13. Dorward DA et al. Tissue-Specific Immunopathology in Fatal COVID-19. *Am. J. Respir. Crit. Care Med.* 2021;203(2):192–201.

14. Grommes J, Soehnlein O. Contribution of neutrophils to acute lung injury. *Mol. Med.* 2011;17(3-4):293–307.

15. Cowland JB, Borregaard N. Granulopoiesis and granules of human neutrophils. *Immunol. Rev.* 2016;273(1):11–28.

16. Borregaard N, Sehested M, Nielsen BS, Sengeløv H, Kjeldsen L. Biosynthesis of granule proteins in normal human bone marrow cells. Gelatinase is a marker of terminal neutrophil differentiation. *Blood* 1995;85(3):812–817.

17. Tyanova S et al. The Perseus computational platform for comprehensive analysis of (prote)omics data. *Nat. Methods* [published online ahead of print: June 27, 2016]; doi:10.1038/nmeth.3901

18. Wiśniewski JR, Hein MY, Cox J, Mann M. A "Proteomic Ruler" for Protein Copy Number and Concentration Estimation without Spike-in Standards. *Mol Cell Proteomics* 2014;13(12):3497–3506.

19. Huang DW, Sherman BT, Lempicki RA. Bioinformatics enrichment tools: paths toward the comprehensive functional analysis of large gene lists. *Nucleic Acids Res.* 2009;37(1):1–13.

20. Huang DW, Sherman BT, Lempicki RA. Systematic and integrative analysis of large gene lists using DAVID bioinformatics resources. *Nat Protoc* 2009;4(1):44–57.

21. Dorward DA et al. The role of formylated peptides and formyl peptide receptor 1 in governing neutrophil function during acute inflammation. *Am. J. Pathol.* 2015;185(5):1172–1184.

22. Silveira AAA et al. TNF induces neutrophil adhesion via formin-dependent cytoskeletal reorganization and activation of β-integrin function. *Journal of Leukocyte Biology* 2018;103(1):87–98.

23. McLeish KR et al. Frontline Science: Tumor necrosis factor-α stimulation and priming of human neutrophil granule exocytosis. *Journal of Leukocyte Biology* 2017;102(1):19–29.

24. Murray J et al. Regulation of neutrophil apoptosis by tumor necrosis factor-alpha: requirement for TNFR55 and TNFR75 for induction of apoptosis in vitro. *Blood* 1997;90(7):2772–2783.

25. Ramadass M, Johnson JL, Catz SD. Rab27a regulates GM-CSF-dependent priming of neutrophil exocytosis. *Journal of Leukocyte Biology* 2017;101(3):693–702.

26. Kobayashi SD, Voyich JM, Whitney AR, DeLeo FR. Spontaneous neutrophil apoptosis and regulation of cell survival by granulocyte macrophage-colony stimulating factor. *Journal of Leukocyte Biology* 2005;78(6):1408–1418.

27. Faurschou M, Borregaard N. Neutrophil granules and secretory vesicles in inflammation. *Microbes and Infection* 2003;5(14):1317–1327.

28. Garnett JP et al. Proinflammatory mediators disrupt glucose homeostasis in airway surface liquid. *J. Immunol.* 2012;189(1):373–380.

29. Mallia P et al. Role of airway glucose in bacterial infections in patients with chronic obstructive pulmonary disease. *J. Allergy Clin. Immunol.* 2018;142(3):815–823.e6.

30. Bhutia YD, Ganapathy V. Glutamine transporters in mammalian cells and their functions in physiology and cancer. *Biochim. Biophys. Acta* 2016;1863(10):2531–2539.

31. Commisso C et al. Macropinocytosis of protein is an amino acid supply route in Ras-transformed cells. *Nature* 2013;497(7451):633–637.

32. Palm W et al. The Utilization of Extracellular Proteins as Nutrients Is Suppressed by mTORC1. *Cell* 2015;162(2):259–270.

33. Davidson SM et al. Direct evidence for cancer-cell-autonomous extracellular protein catabolism in pancreatic tumors. *Nat. Med.* 2017;23(2):235–241.

34. Sadiku P et al. Neutrophils Fuel Effective Immune Responses through Gluconeogenesis and Glycogenesis. *Cell Metabolism* 2021;33(2):411–423.e4.

35. Recouvreux MV, Commisso C. Macropinocytosis: A Metabolic Adaptation to Nutrient Stress in Cancer. *Front Endocrinol (Lausanne)* 2017;8:261.

36. Canton J et al. Calcium-sensing receptors signal constitutive macropinocytosis and facilitate the uptake of NOD2 ligands in macrophages. *Nat Commun* 2016;7(1):11284.

37. Sancak Y et al. Ragulator-Rag complex targets mTORC1 to the lysosomal surface and is necessary for its activation by amino acids. *Cell* 2010;141(2):290–303.

38. Choi YJ et al. Inhibitory effect of mTOR activator MHY1485 on autophagy: suppression of lysosomal fusion. *PLoS ONE* 2012;7(8):e43418.

39. Schröder BA, Wrocklage C, Hasilik A, Saftig P. The proteome of lysosomes. *Proteomics* 2010;10(22):4053–4076.

40. Wibo M, Poole B. Protein degradation in cultured cells. II. The uptake of chloroquine by rat fibroblasts and the inhibition of cellular protein degradation and cathepsin B1. *J. Cell Biol.* 1974;63(2 Pt 1):430–440.

41. Neeley SP et al. Selective regulation of expression of surface adhesion molecules Mac-1, L-selectin, and VLA-4 on human eosinophils and neutrophils. *Am J Respir Cell Mol Biol* 1993;8(6):633–639.

42. in 't Veen JC et al. CD11b and L-selectin expression on eosinophils and neutrophils in blood and induced sputum of patients with asthma compared with normal subjects. *Clin. Exp. Allergy* 1998;28(5):606–615.

43. Shen H et al. Chloroquine attenuates paraquat-induced lung injury in mice by altering inflammation, oxidative stress and fibrosis. *Int. Immunopharmacol.* 2017;46:16–22.

44. Zhang L et al. Chloroquine relieves acute lung injury in rats with acute hemorrhagic necrotizing pancreatitis. *J. Huazhong Univ. Sci. Technol. Med. Sci.* 2013;33(3):357–360.

45. Hidalgo A, Chilvers ER, Summers C, Koenderman L. The Neutrophil Life Cycle. *Trends in Immunology* 2019;40(7):584–597.

46. Jones HA et al. In vivo measurement of neutrophil activity in experimental lung inflammation. *Am. J. Respir. Crit. Care Med.* 1994;149(6):1635–1639.

47. Eales KL, Hollinshead KER, Tennant DA. Hypoxia and metabolic adaptation of cancer cells. *Oncogenesis* 2016;5(1):e190–e190.

48. Hays RC, Mandell GL. PO2, pH, and redox potential of experimental abscesses. *Proc. Soc. Exp. Biol. Med.* 1974;147(1):29–30.

49. Campbell EL et al. Transmigrating neutrophils shape the mucosal microenvironment through localized oxygen depletion to influence resolution of inflammation. *Immunity* 2014;40(1):66–77.

50. Ng CT et al. Synovial tissue hypoxia and inflammation in vivo. *Ann. Rheum. Dis.* 2010;69(7):1389–1395.

51. Harris AJ et al. IL4Rα Signaling Abrogates Hypoxic Neutrophil Survival and Limits Acute Lung Injury Responses In Vivo. *Am. J. Respir. Crit. Care Med.* 2019;:rccm.201808–1599OC.

52. Walmsley SR et al. Prolyl hydroxylase 3 (PHD3) is essential for hypoxic regulation of neutrophilic inflammation in humans and mice. *J. Clin. Invest.* 2011;121(3):1053–1063.

53. Cox J, Mann M. MaxQuant enables high peptide identification rates, individualized p.p.b.-range mass accuracies and proteome-wide protein quantification. *Nat. Biotechnol.* 2008;26(12):1367–1372.

54. Perez-Riverol Y et al. The PRIDE database and related tools and resources in 2019: improving support for quantification data. *Nucleic Acids Res.* 2019;47(D1):D442–D450.

Figure 1

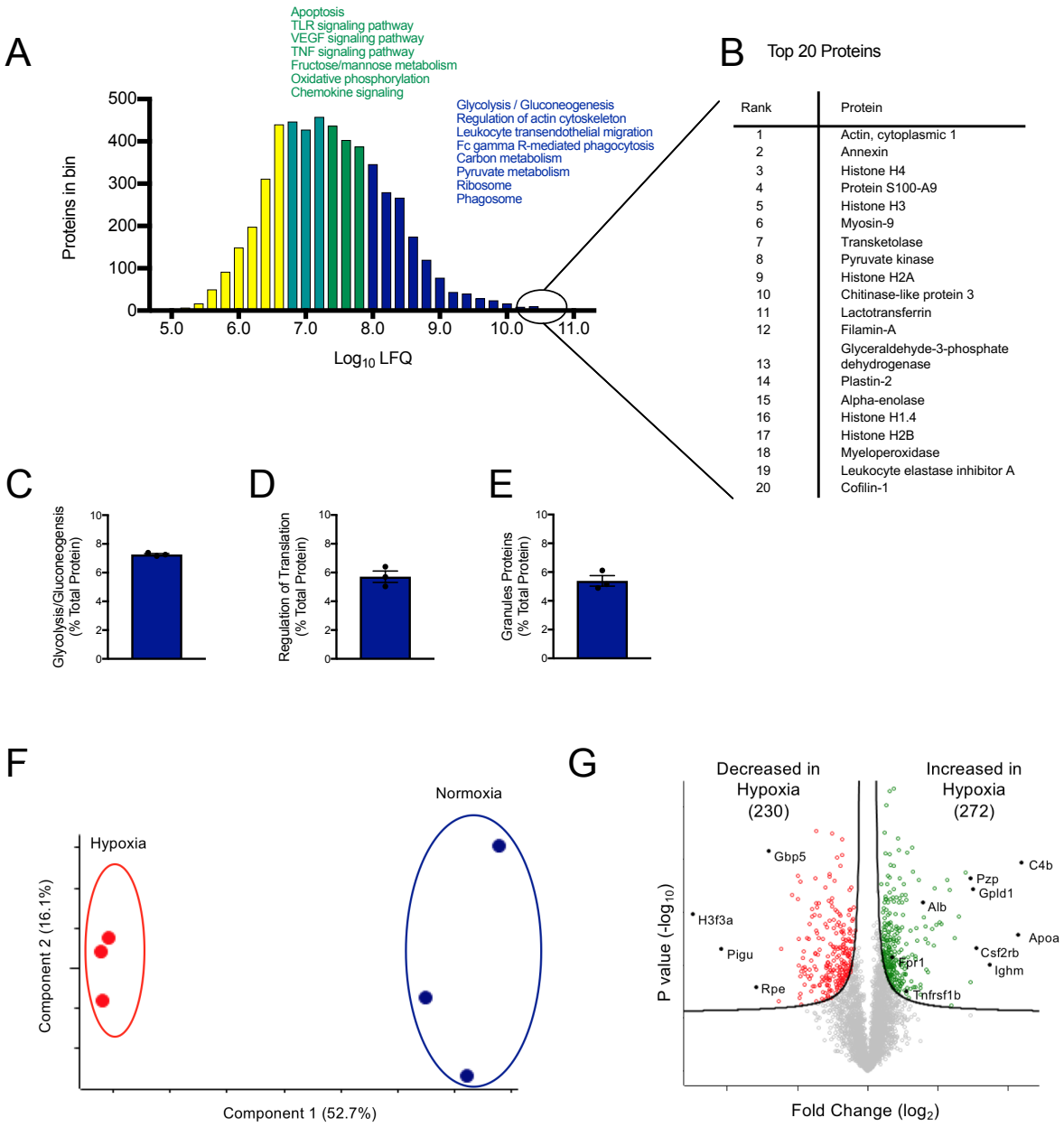

Figure 1: Inflammatory neutrophils re-structure their proteome in response to hypoxia

(A) Histogram of all identified proteins split into quartiles based on label free quantification (LFQ) intensity, KEGG pathway analysis of enriched pathways in the top quartile (dark blue) and 2nd quartile (green) are highlighted. The top 20 proteins (by LFQ intensity) are expanded in (B). The contribution of (C) the Glycolysis/Gluconeogenesis KEGG pathway, (D) the GOBP Regulation of Translation and (E) of granule proteins to the total protein content of a

neutrophil was calculated. The proteome of normoxic and hypoxic BAL neutrophils were analysed for (F) principle component analysis, performed without category enrichment in components. (G) Volcano plot demonstrating significant up-(green) and down-regulation (red) of over 200 proteins in hypoxic samples ($P<0.05$, FDR 0.05, $S_0=0.1$). For all data, n=3 per condition. (D)-(E) represent individual values and mean ± SEM. (F) represents each biological replicate.

Figure 2

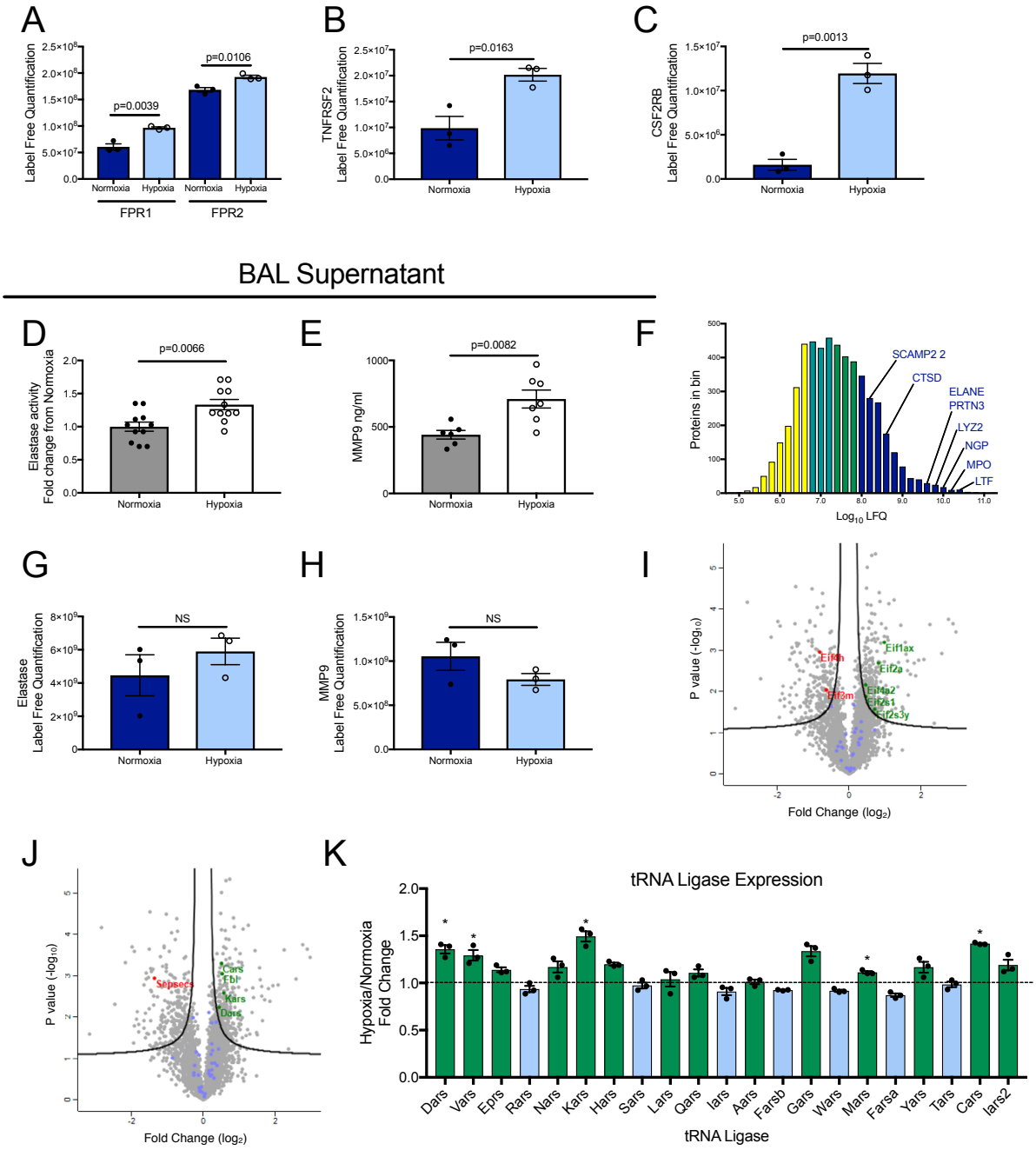

Figure 2: Hypoxia promotes a hyper-inflammatory biosynthetic neutrophil phenotype

Label free quantification of (A) FPRs 1 and 2, (B) TNFRSF2 and (C) GM-CSF receptor subunit β in BAL neutrophils from normoxic and hypoxic mice, n=3. (D) Elastase activity (n=11 over three experiments) and (E) MMP9 concentration (n=6 over two experiments) in BAL supernatant from normoxic and hypoxic mice 6 hours post-LPS, Mann-Whitney test of

significance. (F) Histogram of the normoxic neutrophil proteome with the positions of granule proteins highlighted. Label free quantification of (G) elastase and (H) MMP9 in normoxic and hypoxic BAL neutrophils, n=3. Volcano plots illustrating upregulation of EIFs (I) and tRNA ligases (J) with the fold change of tRNA ligases detailed in (K) with upregulated proteins highlighted in green.

(A)-(C), (G)-(H) and (K) unpaired two tailed t test of significance. (A)-(E)&(G)-(H) Data represents individual values and mean ± SEM. (K) Data represents mean ± SEM.

FPR; formylated peptide receptor, TNFRSF2; TNF receptor superfamily member 2, CSF2RB; GM-CSF receptor subunit β, SCAMP2; Secretory carrier-associated membrane protein 2, CTSD; Cathepsin D, ELANE; Neutrophil Elastase, PRTN3; Myeloblastin (Proteinase 3), LYZ2; Lysozyme C-2, NGP; Neutrophil Granule Protein, MPO; Myeloperoxidase, LTF; Lactotransferrin EIF; Eukaryotic translation initiation factor.

Figure 3

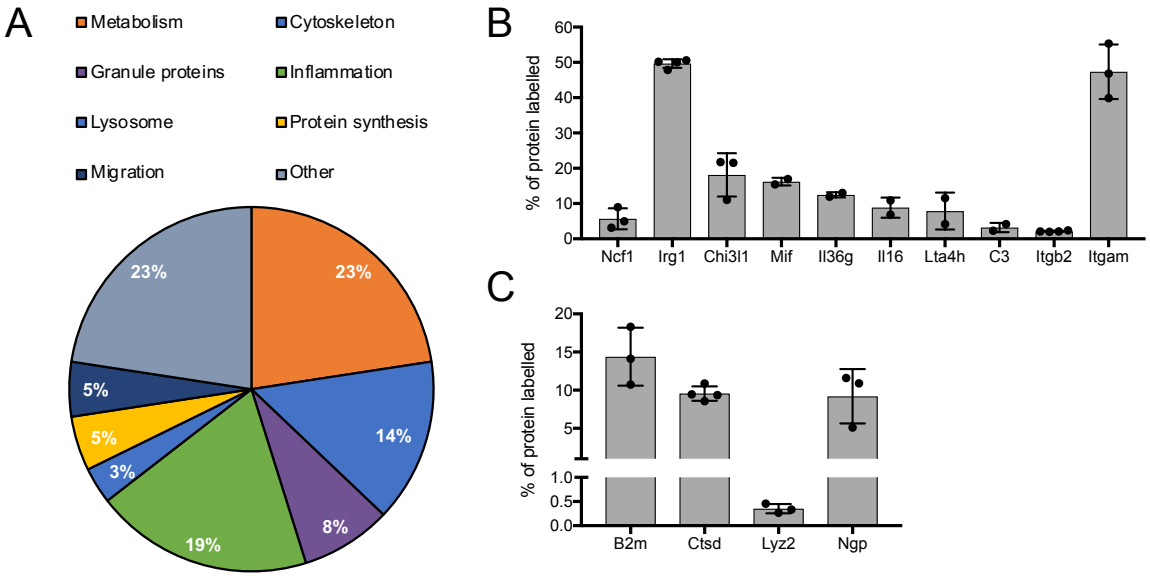

Figure 3: Airspace neutrophils synthesise granule proteins

BAL neutrophils were cultured ex-vivo with labelled amino acids (n=4 over two experiments). Labelled proteins (identified by mass spectrometry, total number =62) were assigned to a functional group as detailed in (A). Those involved in inflammation (B) and neutrophils granules (C) are detailed. (B) and (C) represent individual values and mean ± SEM with labelling expressed as the percentage of that protein which demonstrate in

Figure 4

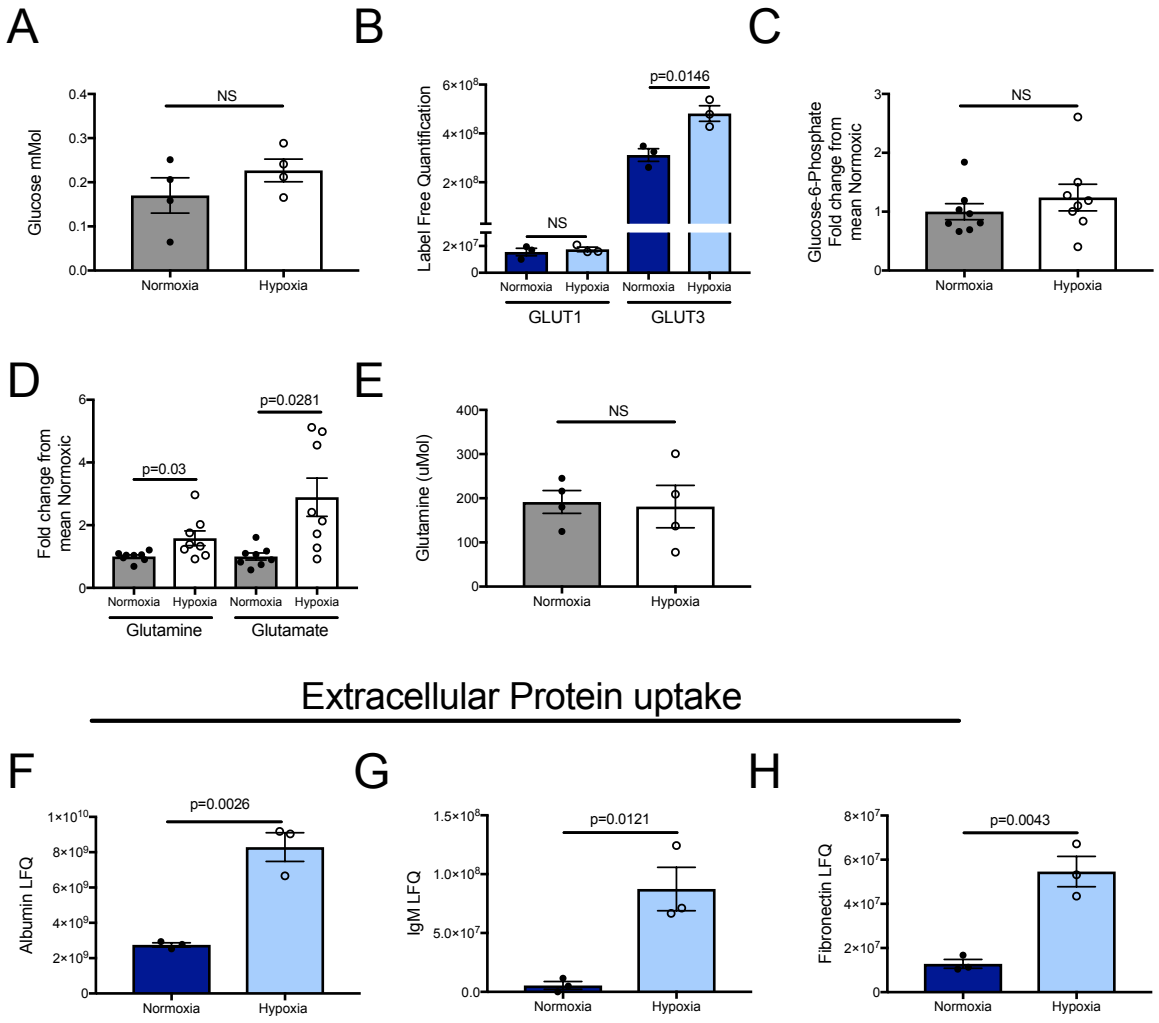

Figure 4: Hypoglycaemic neutrophils scavenge extracellular proteins

(A) Glucose concentration of airway surface liquid (n=4 over one experiment). (B) Label free quantification of glucose transporters GLUT1 and GLUT3, n=3. (C) Intracellular abundance of glucose-6-phosphate measured by HPLC-MS (n=8 over two experiments). (D) Intracellular abundance of glutamate and glutamine (n=8 over two experiments). (E) Glutamine concentration of airway surface liquid from normoxic and hypoxic mice 24 hours post-LPS (n=4 over one experiment). Label free quantification of (F) Albumin, (G) IgM and (H) Fibronectin in BAL neutrophils, n=3. (A) and (C)-(E) Mann-Whitney test of significance.

(B) and (F)-(H) unpaired two tailed t test of significance. All data from normoxic and hypoxic mice 24 hours post nebulised LPS.

Figure 5

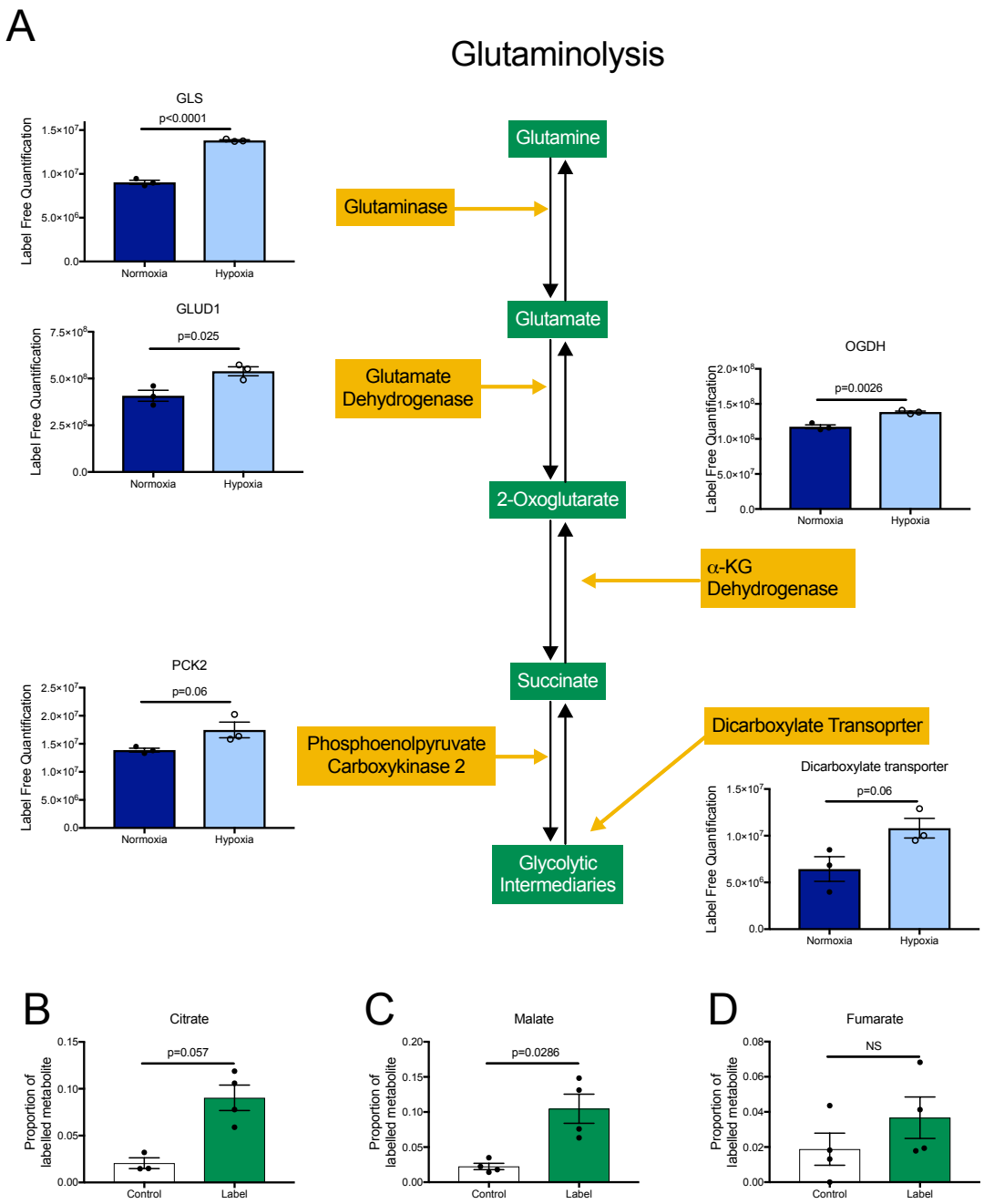

Figure 5: Glutamine from scavenged proteins fuels hypoxic neutrophils

(A) Label free quantification of proteins involved in glutaminolysis, n=3, unpaired two tailed t test of significance. (B)-(D) Highly pure BAL neutrophils harvested 6 hours post-nebulised LPS from hypoxic mice were cultured ex-vivo for 18 hours in hypoxia (1%O_2) in glucose free media supplemented $^{13}C_5$ glutamine labelled (green) or unlabelled (white) HEK cell

lysates. Metabolite abundance and labelling was measured by HPLC-MS (n=4 over two experiments), Mann-Whitney test of significance

Diagram represents the glutaminolysis pathway with enzymes in yellow and metabolic intermediaries in green. (*GLS; Glutaminase, GLUD1; glutamate dehydrogenase 1, OGDH; 2-oxoglutarate dehydrogenase; PCK2; phosphoenolpyruvate carboxykinase*

Figure 6

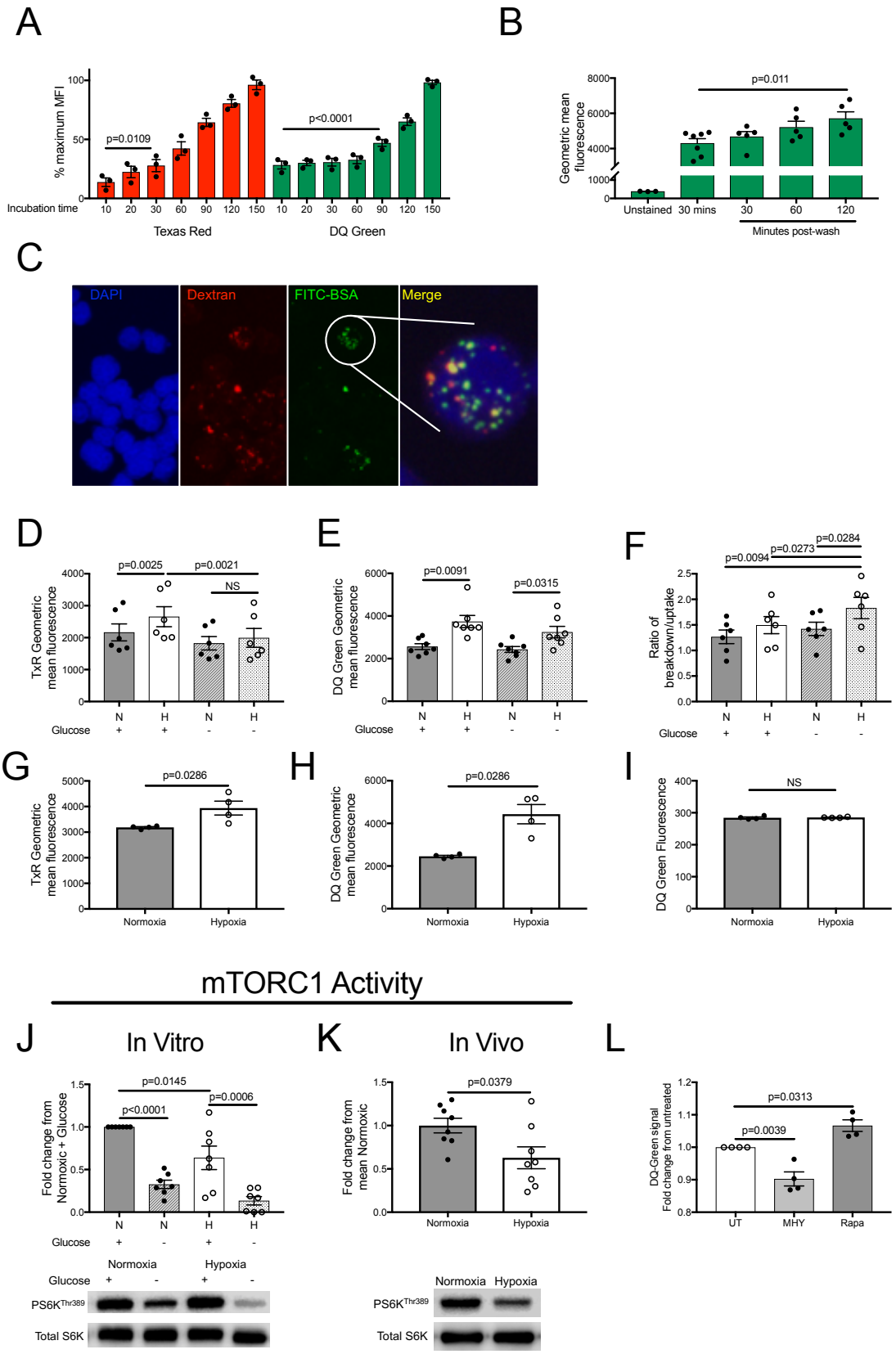
A
% maximum MFI
p=0.0109
p<0.0001
Incubation time
10 20 30 60 90 120 150 10 20 30 60 90 120 150
Texas Red
DQ Green
B
Geometric mean fluorescence
p=0.011
Unstained 30 mins 30 60 120
Minutes post-wash
C
DAPI
Dextran
FITC-BSA
Merge
D
TxR Geometric mean fluorescence
p=0.0025
p=0.0021
NS
N H N H
Glucose + + - -
E
DQ Green Geometric mean fluorescence
p=0.0091
p=0.0315
N H N H
Glucose + + - -
F
Ratio of breakdown/uptake
p=0.0094
p=0.0273
p=0.0284
N H N H
Glucose + + - -
G
TxR Geometric mean fluorescence
p=0.0286
Normoxia
Hypoxia
H
DQ Green Geometric mean fluorescence
p=0.0286
Normoxia
Hypoxia
I
DQ Green Fluorescence
NS
Normoxia
Hypoxia
mTORC1 Activity
J
In Vitro
Fold change from Normoxic + Glucose
p=0.0145
p<0.0001
p=0.0006
N N H H
Glucose + - + -
Normoxia
Hypoxia
Glucose + - + -
PS6K Thr389
Total S6K
K
In Vivo
Fold change from mean Normoxic
p=0.0379
Normoxia
Hypoxia
Normoxia Hypoxia
PS6K Thr389
Total S6K
L
DQ-Green signal Fold change from untreated
p=0.0313
p=0.0039
UT
MHY
Rapa

Figure 6: Hypoxia promotes mTOR regulated neutrophil catabolism of extra-cellular albumin.

Time course of human peripheral blood neutrophils incubated with (A) Texas-red labelled BSA or DQ-Green BSA for 150 minutes (data expressed as % maximum signal) and (B) DQ-Green BSA for 30 minutes followed by washing and then further incubation for 120 minutes, (A)&(B) measured by flow cytometry (n=3 over two experiments). (C) Confocal microscopy of human peripheral blood neutrophils incubated with FITC-BSA (green) and 70kDa dextran (red) with DAPI nuclear staining in blue and red/green co-localisation highlighted in yellow. Geometric mean fluorescence of LPS treated human neutrophils incubated with (D) Texas-Red labelled BSA (n=6) or (E) DQ-Green BSA (n=7 over three experiments) in normoxia or hypoxia (1% O_2) in RPMI ± glucose (11mM). (F) Ratio of DQ-Green to Texas Red signal demonstrating breakdown efficiency in the conditions described in (D) and (E), n=6 over three experiments. Geometric mean fluorescence of BAL neutrophils from normoxic or hypoxic mice 24 hours post-LPS incubated ex-vivo in the corresponding oxygen tension with (G) Texas Red BSA or (H) DQ-Green BSA (n=4 over one experiment). (I) Fluorescence of cell culture supernatant from (H). mTORC1 activity (proportion of phosphorylated S6 kinase) in (J) LPS treated human peripheral blood neutrophils cultured in normoxia or hypoxia (1% O_2) ± glucose (11mM) (n=7 over four experiments) and (K) in murine BAL neutrophils isolated 24 hours post-nebulised LPS (mice housed in normoxia or hypoxia) n=8 over two experiments. Representative blots shown. (L) Geometric mean fluorescence of LPS treated human neutrophils incubated with DQ-Green BSA and pre-treated with MHY1485 (2μM) or Rapamycin (50nM) n=4 over two experiments. (A)&(B) data represents mean ± SEM. (D)-(J) Data represents individual values and mean ± SEM. (A), (B), (D)-(F), (J) and (L) analysed by ordinary one-way ANOVA with multiple comparisons. (G)-(I) & (K) Mann-Whitney test of significance.

Figure 7

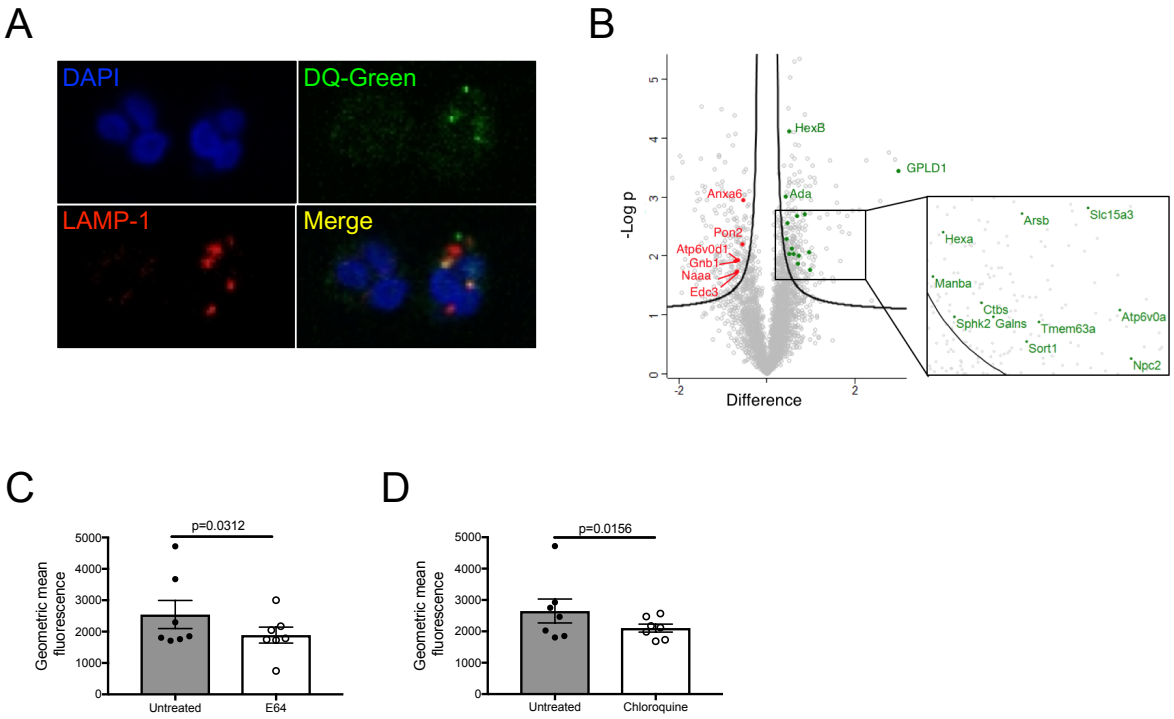

Figure 7: Lysosomal catabolism of extracellular protein provides substrate for de novo protein synthesis

(A) Confocal microscopy of human peripheral blood neutrophils incubated with DQ-Green BSA (green) and subsequently fixed and permeabilised and stained for the lysosomal marker LAMP-1 (red) with DAPI nuclear staining in blue and red/green colocalisation highlighted in yellow. (B) Volcano plot comparing the proteomes of hypoxic and normoxic neutrophils (as in Fig 1H) with lysosomal pathway members which are significantly up- (green) and down-regulated (red) highlighted. Geometric mean fluorescence of LPS treated human neutrophils incubated with DQ-Green BSA and pre-treated with (C) protease inhibitor E64 or (D) the inhibitor of lysosomal acidification chloroquine. n=7 over four experiments, Wilcoxon 2-tailed test of statistical significance. (C)-(D) represent individual values and mean ± SEM.

Figure 8

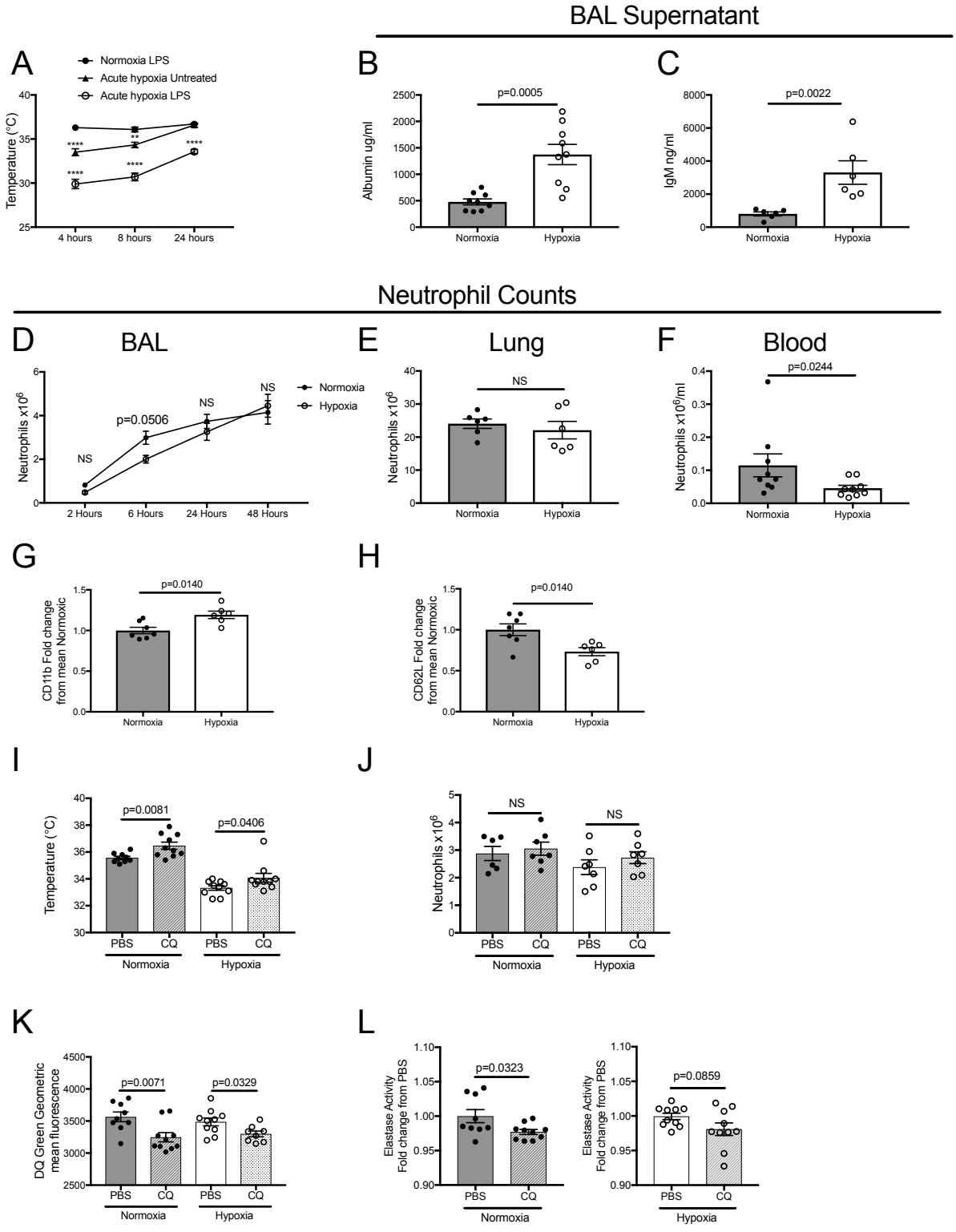
BAL Supernatant
A
Normoxia LPS
Acute hypoxia Untreated
Acute hypoxia LPS
Temperature (°C)
4 hours
8 hours
24 hours
B
Albumin ug/ml
p=0.0005
Normoxia
Hypoxia
C
IgM ng/ml
p=0.0022
Normoxia
Hypoxia
Neutrophil Counts
D
BAL
Neutrophils x10^6
p=0.0506
NS
Normoxia
Hypoxia
2 Hours
6 Hours
24 Hours
48 Hours
E
Lung
Neutrophils x10^6
NS
Normoxia
Hypoxia
F
Blood
Neutrophils x10^6/ml
p=0.0244
Normoxia
Hypoxia
G
CD11b Fold change from mean Normoxic
p=0.0140
Normoxia
Hypoxia
H
CD62L Fold change from mean Normoxic
p=0.0140
Normoxia
Hypoxia
I
Temperature (°C)
p=0.0081
p=0.0406
PBS
CQ
Normoxia
Hypoxia
J
Neutrophils x10^6
NS
NS
PBS
CQ
Normoxia
Hypoxia
K
DQ Green Geometric mean fluorescence
p=0.0071
p=0.0329
PBS
CQ
Normoxia
Hypoxia
L
Elastase Activity Fold change from PBS
p=0.0323
PBS
CQ
Normoxia
p=0.0859
PBS
CQ
Hypoxia

Figure 8: Hypoxia promotes a hyper-inflammatory neutrophil phenotype, abrogated by lysosomal inhibition

(A) Body temperature of mice housed in hypoxia (10% O_2) or normoxia for 24 hours post-nebulised LPS and untreated mice housed in hypoxia, n=4 over two experiments, analysed by two-way ANOVA with Tukey's multiple comparisons test. ** $p<0.01$, **** $p<0.0001$. BAL supernatant from normoxic and hypoxic mice, 24 hours post-LPS was analysed for (B) albumin (n=9 over two experiments) and (C) IgM (n=5 over one experiment) by ELISA. (D) BAL neutrophil counts from normoxic or hypoxic mice following nebulised LPS (n=4 (one experiment) at 2 and 48-hour timepoints, n=8 (two experiments) at 6- and 24-hour time points), significance analysed by multiple t-tests (corrected for multiple comparisons using Bonferroni method). (E) Lung neutrophil counts (n=6 over two experiments) and (F) blood neutrophil counts (n=9 over three experiments) of mice housed in normoxia or hypoxia for 24 hours following LPS nebulisation. BAL neutrophils isolated 24 hours post-nebulised LPS from normoxic or hypoxic mice were analysed by flow cytometry for expression of (G) CD11b and (H) CD62L (n=6-7 over two experiments). (I) Body temperatures and (J) BAL neutrophil counts from mice 24 hours following LPS nebulisation, treated with IP chloroquine or IP PBS at 4 hours and housed in normoxia or hypoxia. (K) BAL neutrophils incubated ex-vivo with DQ-Green BSA and analysed by flow cytometry and (L) elastase activity in BAL supernatant from the same mice. (I) and (K)-(L) n=9-10 over three experiments, (J) n=6-7 over two experiments. (J), (K) and (L) Unpaired t test. (I) Mann-Whitney test of significance (data not normally distributed). (A) and (D) Data represents mean ± SEM. Data in (B), (C) and (E)-(L) represent individual values and mean ± SEM.